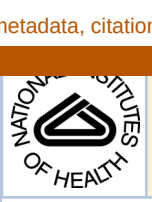

Published in final edited form as:
Circulation. 2011 April 5; 123(13): 1400–1409. doi:10.1161/CIRCULATIONAHA.110.003210.

Stent Thrombogenicity Early in High Risk Interventional Settings is Driven by Stent Design and Deployment, and Protected by Polymer-Drug Coatings

Kumaran Kolandaivelu, MD, PhD[1,2], **Rajesh Swaminathan, MD**[1], **William J. Gibson, BS**[1], **Vijaya B. Kolachalama, PhD**[1], **Kim-Lien Nguyen-Ehrenreich, MS**[3], **Virginia L. Giddings, PhD**[3], **Leslie Coleman, DVM, MS, DACLAM**[3], **Gee K. Wong, BS**[1], and **Elazer R. Edelman, MD, PhD, FACC**[1,2]

[1] Harvard-MIT Division of Health Sciences and Technology, Cambridge, MA

[2] Cardiovascular Division, Brigham and Women's Hospital, Harvard Medical School, Boston, MA

[3] Abbott Vascular, Santa Clara, CA

Abstract

Background—Stent thrombosis is a lethal complication of endovascular intervention. Concern has been raised for the inherent risk associated with specific stent designs and drug-eluting coatings, yet clinical and animal support are equivocal.

Methods and Results—We examined whether drug-eluting coatings are inherently thrombogenic and if the response to these materials was determined to a greater degree by stent design and deployment using custom-built stents. Drug/polymer coatings uniformly reduce rather than increase thrombogenicity relative to matched bare-metal counterparts (0.65-fold, p=0.011). Thick-strutted (162 μm) stents were 1.5-fold more thrombogenic than otherwise identical thin-strutted (81 μm) devices in *ex vivo* flow loops (p<0.001), commensurate with 1.6-fold greater thrombus coverage three days after implantation in porcine coronary arteries (p=0.004). When bare-metal stents were deployed in malapposed or overlapping configurations, thrombogenicity increased compared to apposed, length-matched controls (1.58-fold, p=0.001 and 2.32-fold, p<0.001). The thrombogenicity of polymer-coated stents with thin struts was lowest in all configurations and remained insensitive to incomplete deployment. Computational modeling-based predictions of stent-induced flow derangements correlated with spatial distribution of formed clots.

Conclusions—Contrary to popular conception drug/polymer coatings do not inherently increase acute stent clotting – they reduce thrombosis. However, strut dimensions and positioning relative to the vessel wall are critical factors in modulating stent thrombogenicity. Optimal stent geometries and surfaces, as demonstrated with thin stent struts, help reduce the potential for thrombosis despite complex stent configurations and variability in deployment.

Keywords

stent; thrombosis; hemodynamics; malapposition; overlap

Correspondence to: Kumaran Kolandaivelu, MD, PhD, 77 Massachusetts Avenue, Cambridge, MA 02139, Phone: 617-803-6830, Fax: 617-253-2514, kkolandaivelu@partners.org.

Conflict of Interest Disclosures

Dr. Edelman reports research support from Abbott Vascular, Boston Scientific and Cordis Corporation. L. Coleman and V. Giddings are employees of and have equity interest in Abbott Vascular. K. L. Nguyen-Ehrenreich is an employee of Abbott Vascular. The remaining authors report no conflicts.

Introduction

Stent thrombosis (ST) is a potentially lethal complication of endovascular intervention that arises early after implantation and can persist for years with drug-eluting stents (DES). Steady state risk of ~ 0.6–1% annually[1, 2] is increased by ubiquitous co-morbidities like diabetes mellitus, renal failure, and congestive heart failure,[3–6] and use in arterial bifurcations, long lesions, or overlap.[7–10] Stent-wall malapposition has been observed using intravascular ultrasound (IVUS) in nearly 80% of cases presenting with ST.[7] Importantly, ST incidence increases substantially when multiple risk factors occur simultaneously, exceeding 12% in some analyses.[5]

The issue of device and material biocompatibility is not unique to stents – it is a grander issue and must be perceived as contextual rather than constitutive.[11] Thus, stent geometry, material, and coatings can affect thrombogenicity but it is incumbent upon us to define when and how. Given stent position adjacent to the injured vessel wall and within the flowing bloodstream, it is natural to consider the flow environment, vessel wall, and blood state as contextual elements influencing ST.[12, 13] We evaluated the thrombogenicity of bare and polymer/drug-coated stents using an integrated approach employing *ex vivo*, *in vivo* and *in silico* insights. Well-deployed conformations were compared with high-risk scenarios where stent-induced flow disruptions arise from increased strut dimension, or device malapposition or overlap.

Methods

Ex Vivo Flow Setup

A modified Chandler Loop evaluated endovascular device thrombosis.[14] Motor-controlled rotors accelerate blood-filled silicone loops (Figure 1a; 3.18 mm ID/4.76 mm OD, shore 50A durometer, 3350 Tygon), generating pulsatile flow simulating coronary-like hemodynamics (peak flow 200ml/min).[13, 14] To model wall injury, loop segments were made reactive through 8 hour incubation with 28.3% Bovine Type-I collagen solution (Beckton Dickinson) and subsequently rinsed with PBS, pH~7.4. Stents of different designs were balloon-expanded into the reactive segments under specific deployment configurations (well-apposed, malapposed, or overlapped). Blood was collected from naïve 4-month old Yorkshire pigs (36–40kg) per institutional protocols (Concord Biomedical Sciences & Emerging Technologies) in 10% acid-citrate-dextrose solution (ACD; 85mM trisodium citrate, 69mM citric acid, 111mM glucose, pH~4.6). Prior to use, blood was repleted with a 100mM $CaCl_2$/75mM $MgCl_2$ solution with 62.5μL calcium/magnesium solution per 1mL of blood. Loops were filled, rotor-mounted and run for 4 minutes allowing in-stent thrombus formation. Free blood was emptied and reactive segments isolated and flushed with 120ml Tyrode's solution supplemented with HEPES buffer and magnesium (0.01M HEPES, 0.75mM MgCl2). After visual assessment (Figure 1a), stented segments were excised and filled with 1% Triton-X solution for 20 minutes. Equi-volume lysates were collected and lactate dehydrogenase (LDH) levels determined to provide quantitative measure of platelet/cell adhesion reflecting thrombogenicity (CytoTox 96R Non-Radioactive Cytotoxicity Assay, Promega Corporation).[13, 14]

Ex Vivo Comparisons of Basic Stent Design

ST was evaluated in well-deployed and high-risk scenarios where flow disruptions arise from stent protrusion or device malapposition (Supplemental Material). Stents were pre-mounted on balloon catheters (Abbott Vascular). Bare-metal thin-strut ($81\times81\mu m^2$) stents with a platform identical to clinical MULTI-LINK VISION (MLV) stents were compared to

custom-built non-clinical stents of identical design but two-fold thicker ("THICK-STRUT" VISION; TSV 162×81μm^2) struts (3.0×12mm; N=8 per group). Apposed DES formulated on the thin MLV backbone (XIENCE V, XVS, 96×96μm^2, 3.0×12mm) ran concurrently (N=8) to examine the effect of drug/polymer coatings. A range of clinical-build BMS and DES was also tested. 3.0×12mm BMS (MLV, Driver, TAXUS, Bx VELOCITY; N=6 each) were inflated to 3.2mm and compared to similarly deployed, 3.0×12mm DES counterparts (XVS, Endeavor, TAXUS Liberté, CYPHER; N=6 each). LDH values (in 485nm absorbance) were normalized to MLV data.

Ex Vivo Comparisons of Stent Malapposition and Overlap

Devices were apposed to loop walls or under-expanded to a spectrum of stent:wall separations - 0–60μm (malapposition threshold (MT), 150–210μm (intermediate), or 350–400μm (severe) (Figure 1b–c; Supplemental Material). All stents were fixed within the loops through 15 atm edge inflation. Some MLV stents were fully expanded to 15atm and compared to thin BM (MLV), thick BM (TSV), or thin, drug-eluting (XVS) stents sub-maximally expanded at MT (N=8 per group). Apposed MLV devices were compared to the full spectrum of malapposition (N=8 per group). Other stents were overlapped and compared to length-matched controls (Figure 1d). Three configurations were tested using 3.0×18mm BMS (MLV and TSV) and DES (XVS) such that a 9mm overlapped region was formed, 33% of the total stented 27mm length (N=8 per overlap group). MLV (3.0×28mm, N=8 each) served as single, length-matched controls.

In Vivo Testing: Effect of Strut Thickness

Four Yorkshire swine (40–44kg) were maintained in accordance with Animal Welfare Act and Institutional regulations. Pigs were anesthetized with inhaled isoflurane and local 2% lidocaine. 6Fr femoral arterial access was obtained. Following heparinization, 3.0×12mm stents were deployed into coronary arteries using standard techniques. Single stents (MLV or TSV) were deployed into the left anterior descending (LAD), circumflex (Cx), or right coronary artery (RCA) of each animal - 6 thin or thick stents in 12 vessels. Deployment was staggered with 2 stents of each type in the 3 arterial positions. Animals were maintained on normal pig chow diet and daily aspirin (600mg). Clopidogrel (300mg) was administered pre-intervention. Following the procedure, pigs continued on aspirin (81mg) and clopidogrel (75mg).

After 3 days, animals were euthanized. Stented segments were harvested (N=6 per stent type), fixed in 10% neutral buffered formalin, dehydrated in ethanol, xylene cleared and methyl methacrylate (MMA) resin embedded (Supplemental Material). Blocks were sawed at proximal, mid and distal stent planes. 5μm thicknesses were sectioned and stained with Hematoxylin/Eosin-Y and Verhoeff-vanGieson elastin stains. Luminal thrombus area was quantified and fibrin content scored (0=Absent, 1=Light, 2=Moderate, 3=Heavy with spans between struts) using Adobe Photoshop (Adobe Inc.). Mean values were averaged over the stent length.

Computational Modeling

Flow perturbations induced by 81×81μm^2 or 162×81μm^2 struts (identical to MLV/TSV platforms) were modeled within 3.0mm lumen at graded wall separation (0–320μm and the centerline flow) with 1.5cm entrance and exit lengths. Separately, two 10 strut-long stents with 5 overlapping struts were considered. Overlapping struts were congruent (aligned) or non-congruent (off-set) – where struts lie precisely on top of each other or phase shifted to various degrees as overlapping struts rest between underlying struts.

A finite element-based non-Newtonian fluid dynamic module (COMSOL Inc.) solved the Navier-Stokes equations in the arterial lumen (Supplemental Material). Steady Poiseuille inlet conditions were characterized by typical coronary blood flow and symmetric vessel characteristics (Reynolds number~242).[15, 16] Zero-pressure outlet and no-slip blood-wall interface boundary conditions were imposed. Delaunay triangulation set mesh generation and the Direct (PARDISO) algorithm solved the linear equations. Mesh density increased with successive simulation until less than 2% difference in the mean velocity in the distal recirculation zone. This convergence was achieved after two successive mesh refinements resulting in 35,648 triangular elements. Iterations for each simulation were performed until the weighted Euclidean norm for the estimated relative error became less than 10^{-9}.

Statistical Analysis

All experiments considered apposed MLV stents as a reference facilitating inter-group comparisons. *Ex vivo* LDH data are thus provided as normalized ratios, expressed as mean ± standard deviation. The Anderson-Darling test for normality was performed on all observational groups (Supplemental Material). When sample normality was justified, statistical comparisons between groups were performed using the unpaired Student's t-test assuming unequal variances. When normality could not be supported, the two-sample Mann-Whitney test was employed. Provided p-values were derived from the Student's t-test unless otherwise indicated in the text. Experimental differences were statistically significant at $p<0.05$.

Results

Impact of Basic Stent Features

Thicker stents were 49% more thrombogenic (1.49±0.20, $p<0.001$; Figure 2) and coated stents less thrombogenic than matched MLV BMS (0.76±0.02 vs. 1.00±0.15, p=0.002; Figure 2). These relationships held for stents of different designs. Clot mass remained significantly reduced when all DES were pooled as a group and compared to BMS (0.67±0.35 vs. 1.03±0.54, p=0.011 as determined by the Mann-Whitney test, Figures 3a–b). Thrombogenicity within the various BMS designs correlated with strut thickness (0.88±0.38 for struts < 100μm vs. 1.44±0.65 for struts > 100μm, p=0.036 as determined by the Mann-Whitney test, Figure 3c). These same results were observed *in vivo*. Radiographs of the excised stented coronary arteries confirmed uniform deployment (Figure 4a–b). Thick devices demonstrated significantly more thrombus after 3 days (Figure 4c–d) with 62% more clot than with thinner versions (0.21±0.041 vs. 0.13±0.019mm^2, p=0.004; Figure 4e). Neointimal fibrin accumulated around thick struts more than thin (1.56±0.40 vs. 0.83±0.41, p=0.016 via the Mann-Whitney test) commensurate with the location and extent of flow stagnation and recirculation as determined computationally (3.6-fold downstream and 1.4-fold upstream increase in recirculation area with increasing strut dimension; Figure 4f).

Impact of Suboptimal Stent Deployment: Malapposition

Thin and thick strut stents with 0–60μm wall separation were more thrombogenic than apposed thin strut stents (1.58±0.17 and 1.64±0.17 vs. 1.00±0.27, $p<0.001$; Figure 5a). The slightly malapposed thin-strut stents carried similar thrombotic risk to apposed thick-strut stents (p=ns; Figure 2 and 5). DES coatings which reduced BMS thrombogenicity when apposed continued to limit thrombogenicity malapposed (0.73±0.007, p=0.037). There was no statistical difference between thin DES in apposed and malapposed configurations (p=ns, Figures 2 and 5).

Intriguingly, malapposition could not explain thrombogenicity until the extent and pattern of flow disruption associated with the strut and the wall was introduced. Clot mass was greatest

at mild (1.58±0.17) and severe (1.30±0.10) malapposition, but less so at intermediate strut-wall separation (0.85±0.17; Figure 5b). Strut-induced recirculation changed in size and location depending on wall apposition (Figure 5c, d). Recirculation could appear adjacent to the wall or stent; when the strut was close to the wall, these coincided. As strut-wall separation increased, recirculation zones initially remained on the wall increasing in size. With further displacement, they shifted downstream losing communication with the strut itself. Eventually wall-contacting flow disturbances faded away all together. With greatest wall separation, recirculation reemerged as strut-associated flow disruptions adjacent to and on the downstream aspect of the strut, now apart from the wall and within the flow field.

Impact of Suboptimal Stent Deployment: Overlap

Overlapped BMS were more thrombogenic than single length-matched controls, and more so for thick stents than thin (2.32±0.96 and 3.25±0.11 vs. 1.00±0.17, $p<0.001$ via the Mann-Whitney test; Figure 6a). Moreover, overlapped thin DES (0.51±0.019) were less thrombogenic than overlapped BMS ($p<0.001$) and even single BMS controls ($p<0.001$; both via the Mann-Whitney test). Overlap increases the amount of stent material and recirculation per unit length compared to non-overlapped portions, and more so for thicker struts. Flow was restored between thin struts, and in non-congruent cases where overlap allowed struts of upper stents to fall between struts of lower devices. When overlapping stents were congruent with struts piled one on top of the other, recirculation increased and was massive, spanning the entire overlapped inter-strut regions in thick strut cases (Figure 6b).

Discussion

Stent thrombosis (ST) is catastrophic and it is feared that addition of polymeric coatings and drugs increases thrombotic risk.[6, 17] We now show in a controlled model of early ST that clinically relevant polymer-coated stents are consistently less, not more, thrombogenic than matched bare-metal platforms especially in high risk interventions. More important to ST in our models was the interaction of strut dimension and position relative to the vessel wall and the potential alterations in flow and recirculation that are imposed by the implanted device. *In silico* models allowed us to explore further a wide range of application scenarios and device use combinations, demonstrating how thrombogenicity could be modified by synergistic interactions between stent geometry and the local flow environment.

Effects of strut geometry

The importance of stent design and strut position relative to the vessel wall on thrombogenicity is not unexpected,[12] yet not fully supported by clinical data. Stent implantation alters blood-exposed surfaces and luminal flow while creating a foreign stimulus and nidus for clot.[1, 2, 18] Doubling strut thickness nearly doubles foreign material and increases flow separation, stagnation, and re-attachment (Figures 4f, 5f, 6b). Such flow disruptions should enhance platelet deposition and thrombin and fibrin generation.[19] In ISAR-STEREO[20–22] trials, thin-strut (50μm) stents elicited less restenosis than thick-strut (140μm) BMS, and 96μm everolimus-eluting stents (XVS) were less thrombogenic than 164μm and 132μm paclitaxel-eluting devices (3% to 0.7%, $p=0.003$ and 1.1% to 0.3%, $p=0.004$ respectively) in the SPIRIT IV[17] and COMPARE[23] trials. The latter studies implicate strut dimension in ST but as they considered devices differing not only in thickness but in delivered drug, elution kinetics, geometric design, material composition and coating, they do not prove correlation. Indeed, when stents releasing rapamycin-like drugs were compared clinically, thin platforms with rapid elution were not consistently better than thicker, slow-release devices.[24–26] Our work illuminates the impact of strut dimension on ST as an isolated parameter and begins to explain these seemingly ambiguous and even

contradictory clinical findings by incorporating other aspects of stent design and the context in which the designs are deployed.

Material effects

Bare-metal thrombogenicity has long been recognized.[12, 27] Metals may possess high surface potentials that promote thrombus formation while corrosion can activate platelets and pro-inflammatory pathways.[28–31] Well-designed polymer coatings serve as corrosive barriers and provide thromboresistance through modification of properties such as surface potential, wettability, and roughness.[30–32] Yet, polymer coatings are often perceived to be less thromboresistant and less durable than metal, and remain long after drug release is complete. That polymer coatings lowered thrombotic potential as compared to BMS in our ST model, even in the face of challenging deployment, requires explanation.

In the pre-drug eluting era, we found hydrophobic polymer application to BMS reduced 14-day thrombotic occlusion rate from 15% to 0% ($p<0.01$) in a rabbit iliac artery.[12] Fluoropolymeric material and Dacron large artery bypass grafts offer clinical patency similar to venous conduits early in their use.[32, 33] Some analyses of clinical ST suggest reduction in DES-related events as compared to BMS shortly after implantation[1] and other studies failed to show substantial differences between DES and BMS thrombosis rates.[34] Despite possible reduction of *early* thrombogenicity with polymeric material, fear of DES thrombosis is driven largely by *late* events where poor re-re-endothelialization, drug-induced tissue factor expression, inflammation, polymer degradation and hypersensitivity, and late acquired malapposition are observed.[1, 2, 35] Richer definitions of biocompatibility must therefore be invoked to explain clinical DES findings. Although polymer coatings can be thromboresistant, thrombogenicity arises from the bioresponsiveness of time-variant, environments and longitudinal ST risk is a balance of material, flow, and vascular characteristics and responses. Considering the entire context is critical.

Effect of poor deployment

Strut malapposition and stent overlap are associated with ST.[7] IVUS studies of older generation stents reported stent-wall malapposition rates exceeding 20% and more recently 88% of stented lesions had at least one malapposed strut when examined with optical coherence tomography (OCT).[36] Malapposition can occur from inadequate deployment, regression of interposed thrombus, or positive tissue remodeling inferior to the strut. Despite efforts to reduce incomplete deployment, the asymmetric and calcific nature of atherosclerotic lesions alone challenges stent positioning and some variation in placement is inevitable. Though newer platforms, evolving implantation techniques[37] and imaging tools[38, 39] reduce malapposition, recent meta-analyses show that DES as a group have more late stent malapposition compared with BMS.[35] When present, poor apposition increased ST risk over six-fold.[35]

Many cases of ST have some malapposition, but most malapposition does not result in thrombosis.[35, 36] In our models malapposition alone could not account for thrombogenicity. Clot mass increased most when struts were displaced a distance similar to the overall strut height. As strut-wall separation grew, thrombogenicity fell and then increased again as struts were displaced far into the flow field. Computational models validated that strut position in the flow field significantly affects patterns of recirculation and stagnation. The shifting flow patterns observed, coupled with respective thrombogenicities of the stent material and vessel wall, may account for variable reports of ST. Large recirculating wall-contacting flows may promote clot when the vessel wall is prothrombotic, as when necrotic, poorly re-endothelialized, or rich in tissue-factor expression. As struts move further into the freestream, flow recirculation between the strut and wall ceases, maximizing convective

wall transport and then ST is the balance of blood interaction with the stent material and flow alterations induced in the stream (Figure 5d).

As many as 30% of endovascular interventions receive multiple overlapping stents, increasing the mass of foreign material, surface area for clot formation, and likelihood of malapposition.[9, 35, 40] Upper stents cannot be flush to the wall without excessive embedding of the lower device. If lower devices are apposed, the upper stent will protrude significantly into the flow field to an extent directly related to strut dimension. Our data confirm overlap-associated ST risk, correlate strut protrusion with flow alteration and demonstrate the exacerbation of effect with precise stent overlap alignment. When stents perfectly align, struts lay precisely one on top of another and generate maximal flow disruption – when alignment is out of phase, extent of flow separation is minimized. Real-life scenarios attain a spectrum of strut positions relative to other overlapped struts, and here the importance of dimensions emerge. As strut thickness increases, alignment can induce massive, global recirculation zones in contrast to the local disruptions associated with thin struts. The improvement provided by new generation, thinner devices may be accentuated in such complex settings. In the SPIRIT IV trial, thinner devices performed better than thicker platforms as a whole (HR 0.67) and twice as well in patients receiving multiple stents per lesion (HR 0.33).[17]

Thrombogenicity in context

Williams and others increasingly insist that biological implants can never be inherently *biocompatible*, but rather exhibit *biocompatibility* in specific scenarios.[11] While the former is a constitutive, intrinsic property of the implant, the latter is contextual and dependent on application space. Emerging paradigms require that we define biological reactivity on the basis of specific environments rather than material properties of the implants alone. Indeed, platelet activation on stents of different materials was determined by the flow imposed and drugs applied over the stents and to blood.[13] We now extend this scheme to include feedback effects wherein the implant defines its own context by imposing specific flow disruptions. The size and position of the stents struts relative to the wall and each other impact greatly the extent and position of recirculation and stagnation. This idea potentially explains how minor degrees of malapposition can be insidiously problematic, and in contrast how struts can cross the ostium of a branch vessel unnoticed. It also infers that there may well be multiple modes of ST – those that arise by virtue of thrombopathology associated with flow disruptions and the injured vessel wall, those that arise from flow alterations around stent struts or from some combination of the two. With this in mind, endothelial toxicity, tissue factor activation, altered healing and signaling take on added importance, and issues related to stent deployment become intimately entwined with stent design.

Study Limitations

Ex vivo and computational models add insight into the factors impacting device thrombosis, yet they are simplifications and their relevance to clinical settings must be considered. Flow loops do not account for vascular wall response (for example reendothelialization or inflammation) and non-compliant tubing cannot capture complex biomechanical strut-wall interactions. Future flow models incorporating endothelial and smooth muscle cell linings may offer even further insight. Still, the models allow methodical examination of highly controlled environments not possible through animal or clinical testing alone. 2-D simulations provide a glimpse of three-dimensional, time-varying flow fields, the full characterization of which is beyond the manuscript's scope, but whose elucidation should contribute greatly to future understanding. Our *ex vivo* flow studies were performed using porcine blood not exposed to antithrombotic agents to provide the greatest degree of control. Drugs can reduce clot formation in our system but would cloud the central focus of these

investigations. Moreover, assessment of thrombus was not fully blinded as quantifying clot required stent handling and visualization. Finally, the LDH-based assay provides a sensitive, but not specific marker of cellular material. Although LDH signal correlates with clot weight, the contribution from fibrin formation versus platelet accumulation is not characterized. Such mechanistic understanding could help tailor stent and environment-specific drug therapies.

Conclusions

ST is a feared and fatal complication. Concerns that polymer-drug coatings are inherently thrombogenic however must be reconsidered as early clotting is reduced by polymer-drug coatings. Strut dimensions are associated with ST especially in high-risk deployment configurations but inadequate deployment is not directly causal of ST or pathogenic until one appreciates the flow disruption imposed by strut position. Flow tracking can bring together seemingly disparate data regarding thrombosis and deployment, provide clinical tools for optimal placement, direct choice of adjunctive medical therapy and drive future stent design. Optimal designs are likely those that perform well despite inevitable variability in deployment, and characterizing the flow-impact of device placement may more appropriately define thrombotic risk.

Supplementary Material

Refer to Web version on PubMed Central for supplementary material.

Acknowledgments

The authors acknowledge Alex Ma, Yen Chen, Steve Hsu and Shawn Chin Quee for their contributions to this work in stent preparation, flow loop data collection, as well as histological specimen processing. The authors thank Tecplot Inc. for generously providing software license for data visualization.

Sources of Funding

This work was supported in part by a grant from the NIH to ERE (R01 GM 49039) and an unrestricted gift from Abbott Vascular.

References

1. Windecker S, Meier B. Late coronary stent thrombosis. Circulation. 2007; 116:1952–1965. [PubMed: 17965406]
2. Nakazawa G, Finn AV, Joner M, Ladich E, Kutys R, Mont EK, Gold HK, Burke AP, Kolodgie FD, Virmani R. Delayed arterial healing and increased late stent thrombosis at culprit sites after drug-eluting stent placement for acute myocardial infarction patients: An autopsy study. Circulation. 2008; 118:1138–1145. [PubMed: 18725485]
3. Biondi-Zoccai GG, Lotrionte M, Agostoni P, Abbate A, Fusaro M, Burzotta F, Testa L, Sheiban I, Sangiorgi G. A systematic review and meta-analysis on the hazards of discontinuing or not adhering to aspirin among 50,279 patients at risk for coronary artery disease. Eur Heart J. 2006; 27:2667–2674. [PubMed: 17053008]
4. Angiolillo DJ, Fernandez-Ortiz A, Bernardo E, Ramirez C, Sabate M, Jimenez-Quevedo P, Hernandez R, Moreno R, Escaned J, Alfonso F, Banuelos C, Costa MA, Bass TA, Macaya C. Clopidogrel withdrawal is associated with proinflammatory and prothrombotic effects in patients with diabetes and coronary artery disease. Diabetes. 2006; 55:780–784. [PubMed: 16505243]
5. Baran KW, Lasala JM, Cox DA, Song A, Deshpande MC, Jacoski MV, Mascioli SR. A clinical risk score for prediction of stent thrombosis. Am J Cardiol. 2008; 102:541–545. [PubMed: 18721509]
6. Iakovou I, Schmidt T, Bonizzoni E, Ge L, Sangiorgi GM, Stankovic G, Airoldi F, Chieffo A, Montorfano M, Carlino M, Michev I, Corvaja N, Briguori C, Gerckens U, Grube E, Colombo A.

Incidence, predictors, and outcome of thrombosis after successful implantation of drug-eluting stents. JAMA. 2005; 293:2126–2130. [PubMed: 15870416]

7. Cook S, Wenaweser P, Togni M, Billinger M, Morger C, Seiler C, Vogel R, Hess O, Meier B, Windecker S. Incomplete stent apposition and very late stent thrombosis after drug-eluting stent implantation. Circulation. 2007; 115:2426–2434. [PubMed: 17485593]
8. Marroquin OC, Selzer F, Mulukutla SR, Williams DO, Vlachos HA, Wilensky RL, Tanguay JF, Holper EM, Abbott JD, Lee JS, Smith C, Anderson WD, Kelsey SF, Kip KE. A comparison of bare-metal and drug-eluting stents for off-label indications. N Engl J Med. 2008; 358:342–352. [PubMed: 18216354]
9. Shinke T, Li J, Chen JP, Pendyala L, Goodchild T, Jabara R, Geva S, Ueno T, Chronos N, Robinson K, Hou D. High incidence of intramural thrombus after overlapping paclitaxel-eluting stent implantation: Angioscopic and histopathologic analysis in porcine coronary arteries. Circ Cardiovasc Interv. 2008; 1:28–35. [PubMed: 20031652]
10. Lee CW, Kang SJ, Park DW, Lee SH, Kim YH, Kim JJ, Park SW, Mintz GS, Park SJ. Intravascular ultrasound findings in patients with very late stent thrombosis after either drug-eluting or bare-metal stent implantation. J Am Coll Cardiol. 2010; 55:1936–1942. [PubMed: 20430265]
11. Williams DF. On the mechanisms of biocompatibility. Biomaterials. 2008; 29:2941–2953. [PubMed: 18440630]
12. Rogers C, Edelman ER. Endovascular stent design dictates experimental restenosis and thrombosis. Circulation. 1995; 91:2995–3001. [PubMed: 7796511]
13. Kolandaivelu K, Edelman ER. Environmental influences on endovascular stent platelet reactivity: An in vitro comparison of stainless steel and gold surfaces. J Biomed Mater Res A. 2004; 70:186–193. [PubMed: 15227663]
14. Kolandaivelu K, Edelman ER. Low background, pulsatile, in vitro flow circuit for modeling coronary implant thrombosis. J Biomech Eng. 2002; 124:662–668. [PubMed: 12596633]
15. Kolachalama VB, Tzafriri AR, Arifin DY, Edelman ER. Luminal flow patterns dictate arterial drug deposition in stent-based delivery. J Control Release. 2009; 133:24–30. [PubMed: 18926864]
16. Kolachalama VB, Levine EG, Edelman ER. Luminal flow amplifies stent-based drug deposition in arterial bifurcations. PLoS One. 2009; 4:e8105. [PubMed: 19956555]
17. Stone GW, Rizvi A, Newman W, Mastali K, Wang JC, Caputo R, Doostzadeh J, Cao S, Simonton CA, Sudhir K, Lansky AJ, Cutlip DE, Kereiakes DJ. Everolimus-eluting versus paclitaxel-eluting stents in coronary artery disease. N Engl J Med. 2010; 362:1663–1674. [PubMed: 20445180]
18. Chan MY, Weitz JI, Merhi Y, Harrington RA, Becker RC. Catheter thrombosis and percutaneous coronary intervention: Fundamental perspectives on blood, artificial surfaces and antithrombotic drugs. J Thromb Thrombolysis. 2009; 28:366–380. [PubMed: 19597766]
19. Duraiswamy N, Cesar JM, Schoephoerster RT, Moore JE Jr. Effects of stent geometry on local flow dynamics and resulting platelet deposition in an in vitro model. Biorheology. 2008; 45:547–561. [PubMed: 19065004]
20. Moliterno DJ. Restenosis following thin-strut bare-metal stents versus thick-strut drug-eluting stents. Catheter Cardiovasc Interv. 2007; 69:799–800. [PubMed: 17377984]
21. Pache J, Kastrati A, Mehilli J, Schuhlen H, Dotzer F, Hausleiter J, Fleckenstein M, Neumann FJ, Sattelberger U, Schmitt C, Muller M, Dirschinger J, Schomig A. Intracoronary stenting and angiographic results: Strut thickness effect on restenosis outcome (isar-stereo-2) trial. J Am Coll Cardiol. 2003; 41:1283–1288. [PubMed: 12706922]
22. Kastrati A, Mehilli J, Dirschinger J, Dotzer F, Schuhlen H, Neumann FJ, Fleckenstein M, Pfafferott C, Seyfarth M, Schomig A. Intracoronary stenting and angiographic results: Strut thickness effect on restenosis outcome (isar-stereo) trial. Circulation. 2001; 103:2816–2821. [PubMed: 11401938]
23. Kedhi E, Joesoef KS, McFadden E, Wassing J, van Mieghem C, Goedhart D, Smits PC. Second-generation everolimus-eluting and paclitaxel-eluting stents in real-life practice (compare): A randomised trial. Lancet. 2010; 375:201–209. [PubMed: 20060578]
24. Rasmussen K, Maeng M, Kaltoft A, Thayssen P, Kelbaek H, Tilsted HH, Abildgaard U, Christiansen EH, Engstrom T, Krusell LR, Ravkilde J, Hansen PR, Hansen KN, Abildstrom SZ,

Aaroe J, Jensen JS, Kristensen SD, Botker HE, Madsen M, Johnsen SP, Jensen LO, Sorensen HT, Thuesen L, Lassen JF. Efficacy and safety of zotarolimus-eluting and sirolimus-eluting coronary stentsin routine clinical care (sort out iii): A randomised controlled superiority trial. Lancet. 2010; 375:1090–1099. [PubMed: 20231034]

25. Byrne RA, Kastrati A, Tiroch K, Schulz S, Pache J, Pinieck S, Massberg S, Seyfarth M, Laugwitz KL, Birkmeier KA, Schomig A, Mehilli J. 2-year clinical and angiographic outcomes from a randomized trial of polymer-free dual drug-eluting stents versus polymer-based cypher and endeavor [corrected] drug-eluting stents. J Am Coll Cardiol. 2010; 55:2536–2543. [PubMed: 20417052]
26. Bryrne RA, Mehilli J, Tiroch K, Schulz S, Pache J, Holle H, Massberg S, Seyfarth M, Birkmeier KA, Laugwitz KL, Schomig A, Herzzentrum D. Everolimus-eluting (xience v) stents versus sirolimus-eluting (cypher) stents in patients with coronary artery disease: Results from a randomized controlled trial. Journal of the American College of Cardiology. 2010; 55:A183.E1717.
27. Ruygrok PN, Serruys PW. Intracoronary stenting. From concept to custom. Circulation. 1996; 94:882–890. [PubMed: 8790021]
28. Sawyer PN, Srinivasan S. The role of electrochemical surface properties in thrombosis at vascular interfaces: Cumulative experience of studies in animals and man. Bull N Y Acad Med. 1972; 48:235–256. [PubMed: 4500642]
29. Vogler EA, Siedlecki CA. Contact activation of blood-plasma coagulation. Biomaterials. 2009; 30:1857–1869. [PubMed: 19168215]
30. Sprague EA, Palmaz JC, Simon C, Watson A. Electrostatic forces on the surface of metals as measured by atomic force microscopy. J Long Term Eff Med Implants. 2000; 10:111–125. [PubMed: 10947625]
31. Gutensohn K, Beythien C, Bau J, Fenner T, Grewe P, Koester R, Padmanaban K, Kuehnl P. In vitro analyses of diamond-like carbon coated stents. Reduction of metal ion release, platelet activation, and thrombogenicity. Thromb Res. 2000; 99:577–585. [PubMed: 10974344]
32. Jordan SW, Chaikof EL. Novel thromboresistant materials. J Vasc Surg. 2007; 45 (Suppl A):A104–115. [PubMed: 17544031]
33. Pereira CE, Albers M, Romiti M, Brochado-Neto FC, Pereira CA. Meta-analysis of femoropopliteal bypass grafts for lower extremity arterial insufficiency. J Vasc Surg. 2006; 44:510–517. [PubMed: 16950427]
34. James SK, Stenestrand U, Lindback J, Carlsson J, Schersten F, Nilsson T, Wallentin L, Lagerqvist B. Long-term safety and efficacy of drug-eluting versus bare-metal stents in sweden. N Engl J Med. 2009; 360:1933–1945. [PubMed: 19420363]
35. Hassan AK, Bergheanu SC, Stijnen T, van der Hoeven BL, Snoep JD, Plevier JW, Schalij MJ, Wouter Jukema J. Late stent malapposition risk is higher after drug-eluting stent compared with bare-metal stent implantation and associates with late stent thrombosis. Eur Heart J. 2010; 31:1172–1180. [PubMed: 19158118]
36. Tanigawa J, Barlis P, Dimopoulos K, Dalby M, Moore P, Di Mario C. The influence of strut thickness and cell design on immediate apposition of drug-eluting stents assessed by optical coherence tomography. Int J Cardiol. 2009; 134:180–188. [PubMed: 18775576]
37. Nakamura S, Hall P, Gaglione A, Tiecco F, Di Maggio M, Maiello L, Martini G, Colombo A. High pressure assisted coronary stent implantation accomplished without intravascular ultrasound guidance and subsequent anticoagulation. J Am Coll Cardiol. 1997; 29:21–27. [PubMed: 8996290]
38. Moussa I, Di Mario C, Reimers B, Akiyama T, Tobis J, Colombo A. Subacute stent thrombosis in the era of intravascular ultrasound-guided coronary stenting without anticoagulation: Frequency, predictors and clinical outcome. J Am Coll Cardiol. 1997; 29:6–12. [PubMed: 8996288]
39. Roy P, Steinberg DH, Sushinsky SJ, Okabe T, Pinto Slottow TL, Kaneshige K, Xue Z, Satler LF, Kent KM, Suddath WO, Pichard AD, Weissman NJ, Lindsay J, Waksman R. The potential clinical utility of intravascular ultrasound guidance in patients undergoing percutaneous coronary intervention with drug-eluting stents. Eur Heart J. 2008; 29:1851–1857. [PubMed: 18550555]
40. Ellis SG, Colombo A, Grube E, Popma J, Koglin J, Dawkins KD, Stone GW. Incidence, timing, and correlates of stent thrombosis with the polymeric paclitaxel drug-eluting stent: A taxus ii, iv,

v, and vi meta-analysis of 3,445 patients followed for up to 3 years. J Am Coll Cardiol. 2007; 49:1043–1051. [PubMed: 17349883]

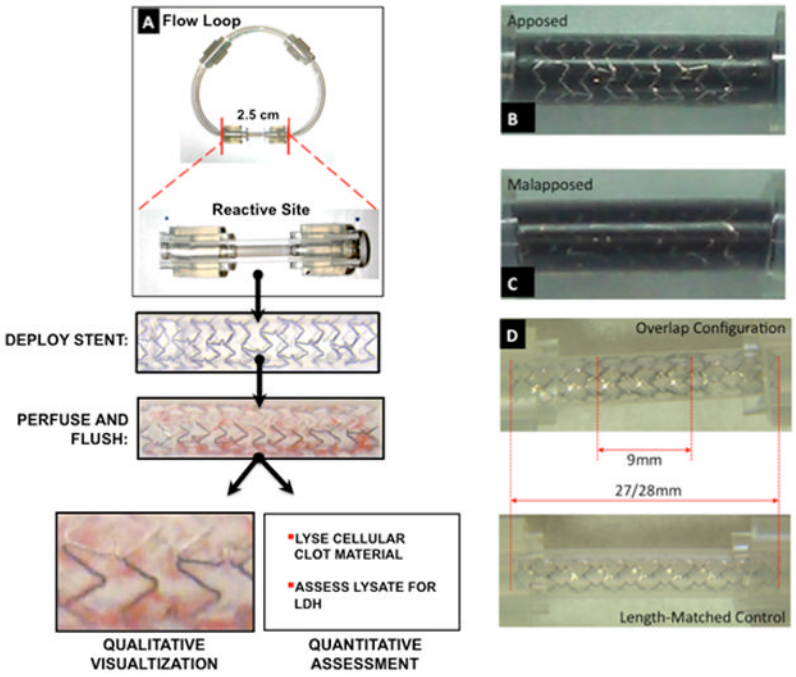

FIGURE 1.

Flow Loop, Reactive Sites, and Stent Configurations. (A) Closed flow loop with a 2.5cm reactive site. Stents are deployed within reactive sites in desired conformations. Following a run, the stented segment is excised and flushed. Adherent clot is assessed visually and through LDH quantification. To determine the malapposition threshold, indigo dye was used to detect stent-wall contact. (B) Proper stent deployment was modeled using apposed configurations. (C) Incomplete stent deployment was modeled using under-deployed configurations. (D) Overlapping stents were compared to length matched controls.

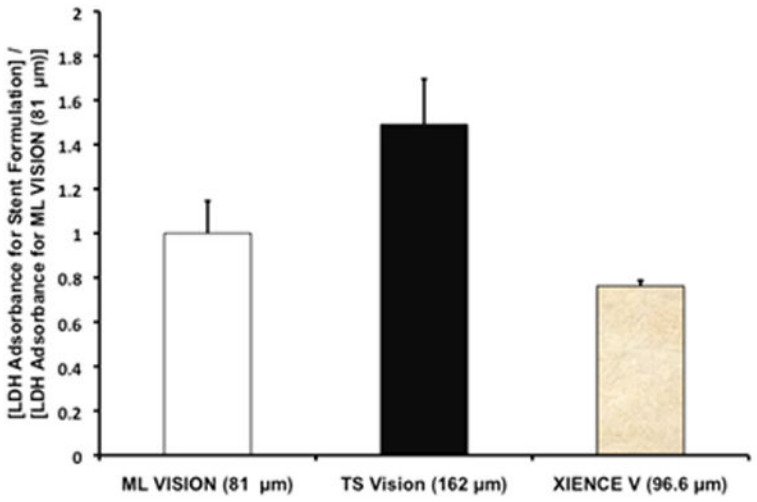

FIGURE 2.
Relative *ex vivo* thrombogenicity between thin BMS (MLV), thick BMS (TSV), and DES (XVS) in apposed configurations.

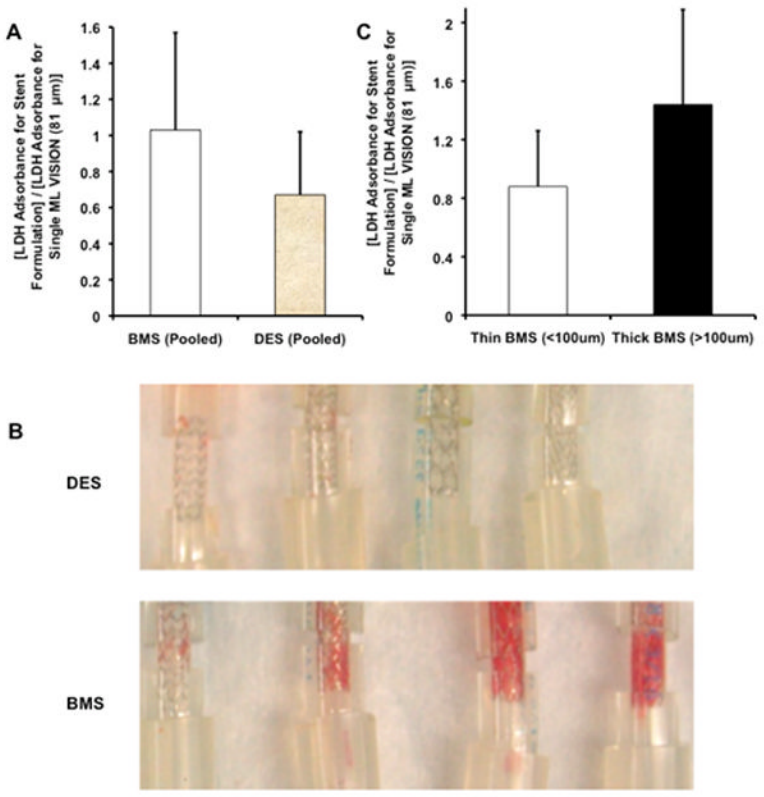

FIGURE 3.

Ex vivo thrombogenicity among BMS and DES of different designs. (A) LDH thrombus quantification and (B) visible clot as observed between pooled DES and BMS designs showing a class effect. (C) LDH quantification in BMS designs grouped according to strut thickness (< 100μm versus > 100μm strut).

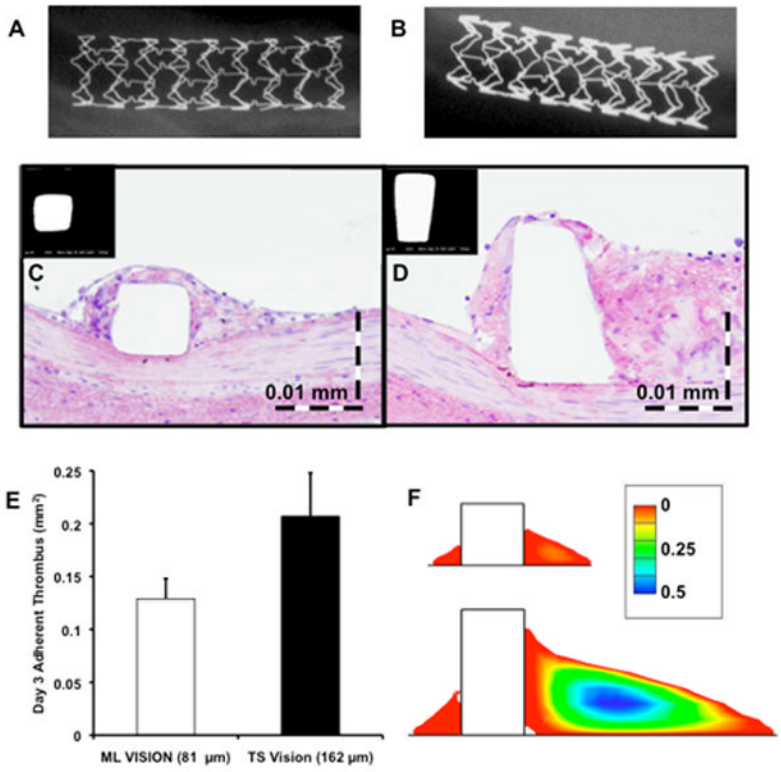

FIGURE 4.

In vivo thrombogenicity of thin (MLV) and thick (TSV) BMS in porcine coronary arteries (n=6 each). (A, B) Radiographs of the excised arteries confirming full expansion of MLV and TSV platforms respectively. (C, D) H&E staining of prepared sections derived from MLV and TSV devices respectively 3 days post-implant. (E) Morphometric analysis of adherent thrombus as assessed through luminal area measurement of MLV and TSV stented sections. (F) Computational models depicting flow alterations surrounding apposed thick (81μm × 162μm) and thin (81μm × 81μm) struts.

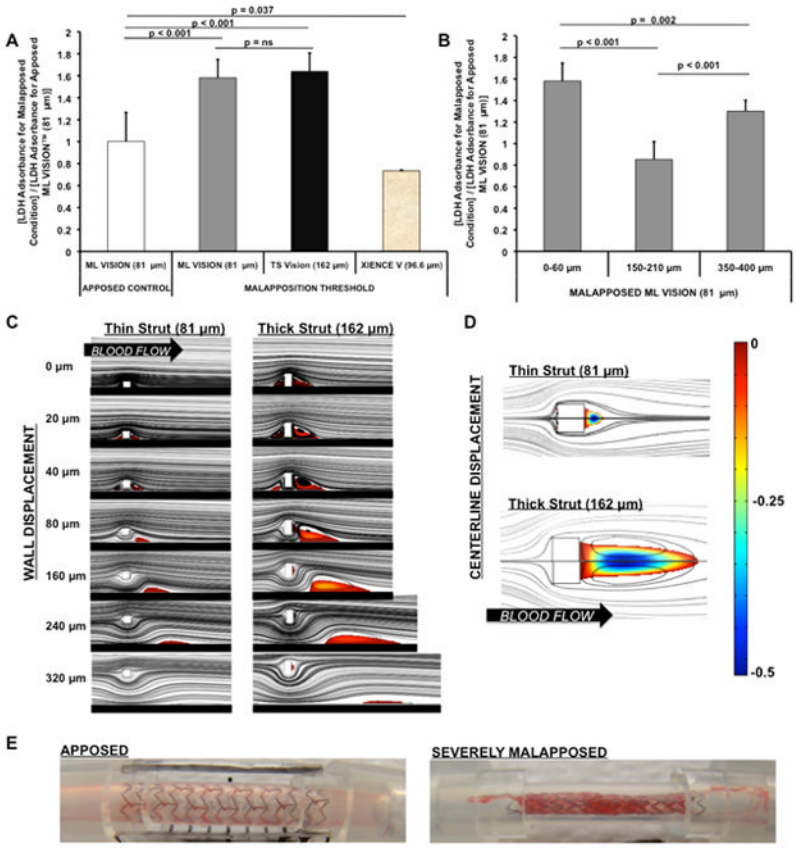

FIGURE 5.

Ex vivo and computational assessment of malapposition cases. (A) Thrombogenicity of thin BMS (MLV), thick BMS (TSV), and DES (XVS) when deployed at their malapposition threshold (0–60µm displacement) as compared to apposed MLV controls. (B) Clot mass in MLV platforms deployed in mild (0–60µm), intermediate (150–210µm), and severe (350–400µm) malapposed configurations showing a variable response. (C) Single strut 2-D simulations with varying displacements showing stent-wall recirculation zones which first grow in size, shift downstream of the stent, lose stent communication, and then fade away altogether. (D) Computed flow pattern with severe wall displacements (shown at the centerline) depicting re-emergence of strut-associated recirculation. (E) Increased visual clot burden observed with severe stent-wall displacement. Depending on the relative thrombogenicities of the wall and the stent, the shifting strut-wall recirculation patterns may help explain variability in malapposition-associated ST events.

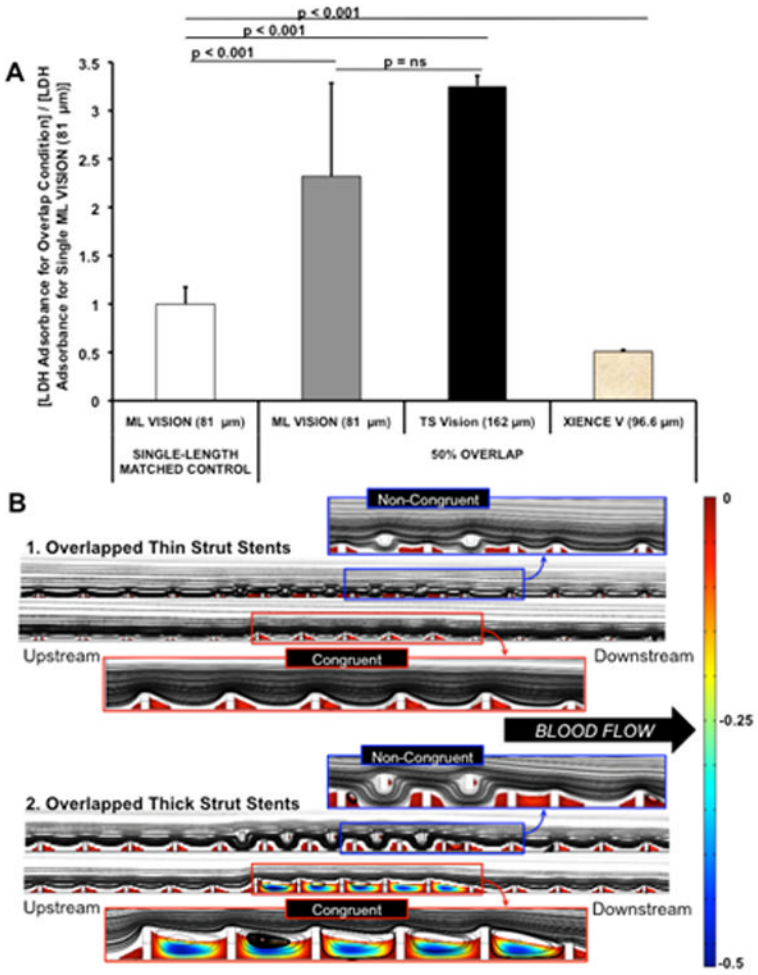

FIGURE 6.

Ex vivo and computational assessment of overlap cases. (A) Thrombogenicity of thin BMS (MLV), thick BMS (TSV), and DES (XVS) when deployed in overlapped configurations as compared with single, length-matched MLV controls. (B) 2-D flow simulations over thin (81μm) and thick (162μm) overlapping stents in congruent or non-congruent configurations. Depending on strut alignment, flow disruptions can be augmented in susceptible geometries (as seen by the recirculation zone spanning the overlapped region in congruent, thick cases).